In Silico Biology 8 (2008) 275–289
IOS Press

Docking-MM-GB/SA and ADME Screening of HIV-1 NNRTI Inhibitor: Nevirapine and its Analogues

Dipankar Sengupta, Deeptak Verma and Pradeep Kumar Naik*

Department of Bioinformatics and Biotechnology, Jaypee University of Information Technology, Waknaghat, Distt.-Solan, Himachal Pradesh, India

Edited by H. Michael; received 15 May 2007; revised 24 April 2008; accepted 7 May 2008; published 5 July 2008

ABSTRACT: Nevirapine and its synthetic analogues, a class of non-nucleoside inhibitors (NNRTIs) of HIV-1 reverse transcriptase (RT), have been the objective of numerous studies focused to prepare better and safer anti-HIV drugs. We developed a library of nevirapine analogues (47) using combinatorial design and with structural modification at X, Y and R substituents in the parent structure of nevirapine. Their molecular interactions and binding affinities with reverse transcriptase (3HVT and 1VRT) have been studied using the docking-molecular mechanics based generalized Born/surface area (MM-GB/SA) solvation model. Final screening of these analogues is based on absorption, distribution, metabolism and excretion (ADME) properties. The proposed NNRTI analogues dock in a similar position and orientation in the active site of RT as co-crystallized nevirapine. In addition a linear correlation was observed between the calculated free energy of binding (FEB) and pIC_{50} for the inhibitors with correlation coefficient R^2 of 0.9948, suggesting that the docked structure orientation and the interaction energies are reasonable. The electrostatic energy terms estimated by GB/SA showed important role on prediction of binding affinity (R^2 = 17.2%). Since we used two different HIV-1 RT crystal structures (3HVT and 1VRT), which are at different resolution (2.9 and 2.2 Å), we propose that structures with resolutions better than 3 Å can be used to produce reasonable docking results. Few analogues showed high binding affinity and activity with RT in compare to co-crystallized nevirapine. These analogues also well qualify ADME properties and showed good druggable characters. The work addressed to modify the X, Y and R substituents in the nevirapine scaffold to prepare synthetic analogues for second generation drug development against RT.

KEYWORDS: HIV-I RT, nevirapine and its analogues, docking, glide, MM-GB/SA, free energy of binding, ADME

INTRODUCTION

The function of the reverse transcriptase of human immunodeficiency virus type 1 (HIV-1 RT) is to transcribe a single-stranded viral RNA genome into double-stranded DNA and plays a vital role in the replication of HIV-1 [1–4]. Several drugs that target this enzyme have been approved to treat Acquired Immune Deficiency Syndrome (AIDS) [5]. There are two types of RT inhibitors. One type is commonly referred to as a nucleoside inhibitor. This inhibitor inserts as nucleoside analogue into DNA and acts as chain-terminating agent, therefore, terminating viral synthesis. The other type is called the non-nucleoside inhibitor (NNRTI) [6–10]. In particular, the non-nucleoside RT inhibitors (NNRTIs) are highly effective and produce few side effects. However, mutations rapidly emerge that confer resistance

*Corresponding author. Tel.: +91 1792 239227; E-mail: pknaik73@rediffmail.com; dipankarsengupta.1982@gmail.com.

Electronic publication can be found in *In Silico Biol.* **8**, 0023 <http://www.bioinfo.de/isb/2008/08/0023/>, 5 July 2008.

to all known NNRTIs, reducing the efficiency of the drugs. It is essential to understand the detailed interactions of the inhibitors with wild type and mutant RT, in order to design more effective drugs.

HIV-1 RT is a protein dimer consisting of two subunits of 66 kDa (p66) and 51 kDa (p51) [7,11–16]. The p66 and p51 subunits are composed of four subdomains called thumb, palm, fingers and connection. The p66 subunit also contains an RNase H domain. NNRTIs bind to a common hydrophobic site, the non-nucleoside inhibitor binding pocket (NNIBP), located in the p66 palm subdomain approximately 10 Å away from the polymerase [1–4]. Numerous crystal structures of RT have been reported, including unliganded, complexed to dsDNA and several NNRTIs. The crystal structures show that all NNRTIs bind to the non-nucleoside inhibitor binding site (NNIBP) in the p66 palm subdomain. Although the overall shape of the NNRTI binding site is very similar amongst the RT/NNRTI complex crystal structures, there are subtle differences among them [17–19]. The amino acid residues composing the non-nucleoside binding site are mainly hydrophobic: Pro95, Leu100, Lys101, Lys103, Val106, Val108, Val179, Tyr181, Tyr188, Gly190, Phe227, Trp229, Leu234, His235, Pro236 and Tyr318 of the p66 palm subdomain (1VRT [20] and 3HVT [21]). There are three water molecules at the entrance of the binding pocket.

Nevirapine and other NNRTIs have demonstrated good activity to inhibit RT. Several crystal structures of NNRTIs/RT complexes have been solved now. It revealed that all NNRTIs bind at the non-nucleoside inhibitor binding site in the p66 palm subdomain. However, the binding mode of many other NNRTI derivatives including nevirapine analogues is not yet known. Although it is assumed that these also bind in a similar mode, there are subtle differences among them [22,23]. Thus, the exploration of the binding mode will provide valuable information to understand the inhibition mechanism of the inhibitors to RT and to help in the design of more potent inhibitors.

Modern approaches for finding new leads for therapeutic targets are increasingly based on 3-dimensional information about receptors. An effective way to predict binding structure of a substrate in its receptor is docking simulation, which has been successfully used in many applications. Some docking methods have demonstrated promising power to predict a reasonable binding structure. Combinations of the method with other methods, such as MD simulation, free energy binding calculation, comparative molecular field analysis (CoMFA) and comparative molecular similarity indices analysis (CoMSIA) enable to get a lot of insights on biological systems and to help rational drug design. Several ways to calculate free energy of binding (FEB) have been suggested and used in different applications. Jorgensen *et al.* [24] have successfully applied Monte Carlo and Linear Response Equation (LRE) on many systems to calculate binding affinities. Wang *et al.* [25] developed the molecular mechanics based poisson-Boltzmann/surface area (MM-PBSA) solvation model and applied the method in the predication of activity of 12 TIBO-like inhibitors. In a free energy calculation, the accurate predictions of solvation and entropy contributions to a binding process are always challenging. Many works have shown that Poisson-Boltzmann and Generalized-Born solvation models are good ways to estimate the electrostatic part of solvation effect in a binding process. Although some work demonstrates that normal mode analysis can be used to estimate the entropy effect in a process, it is very time-consuming.

Recognition by the pharmaceutical industry that undesirable absorption, distribution, metabolism and excretion (ADME) properties of new drug candidates are the cause of many clinical phase drug development failures [26]. This has resulted in a paradigm shift to identify such problems early in the drug discovery process. Thus, *in vitro* approaches are now widely used to investigate the ADME properties of new chemical entities and, more recently, computational (*in silico*) modeling has been investigated as a tool to optimize selection of the most suitable candidates for drug development.

In the present work nevirapine and 47 structural nevirapine derivatives were used to study the binding modes and binding affinities to the receptor; also the free energy of binding was analyzed. We try to

use a flexible docking (Glide) approach to predict the "preferable" binding structure of a ligand in RT. To study the association of the ligands with the receptor further, we use the automated mechanism of Multi-Ligand Bimolecular Association with Energetics (eMBrAcE). It uses traditional MM methods to calculate ligand-receptor interaction energies (electrostatic energy (*Gele*), van der Waals energy (*GvdW*)), with a generalized-Born/surface area (GB/SA) solvation method for electrostatic part of solvation energy (*Gsolv*) [27–29] and solvent-accessible surface for the nonpolar part of solvation energy [30]. The approach is simple, fast and straightforward. It benefits the calculation of relative binding affinity needed to evaluate the activity of large set of molecules in rational drug design. The final screening of the nevirapine and its analogues for the probable absorption, distribution, metabolism and excretion (ADME) properties are calculated using the Qikprop program (Schrödinger, Inc.).

The co-crystallized structure of only the nevirapine (1VRT and 3HVT) with RT is available. However, the effectiveness of other derivatives of nevirapine is yet to be determined. The need to determine their binding structures in the active site of RT and explore the interactions for these new RT analogues is essential in order to improve the design of second generation inhibitors. Hence, in this study we have set out to study the binding mode of nevirapine and its analogues using a combined approach of docking-MM-GB/SA and their final screening based on ADME properties, leading to successful drug development.

MATERIALS AND METHODS

Preparation of protein target structure

The starting coordinates of the HIV-1 RT [1VRT and 3HVT] were taken from the Protein Data Bank (www.rcsb.org) and further modified to be used for Glide docking (Schrödinger, Inc.). The complex were imported to maestro window (Schröger, Inc.), the co-crystallized ligands were identified and removed from the structure and the protein was minimized using the protein preparation wizard (shipped by Schrödinger) by applying OPLS_2005 force field by application of the autoref.pl script. Progressively weaker restraints (tethering force constants 3, 1, 0.3, 0.1) were applied to nonhydrogen atoms only. This refinement procedure is recommended by Schrödinger (technical notes for version 1.8), because Glide uses the full OPLS-AA force field at an intermediate docking stage and is claimed to be more sensitive towards geometric details than other docking tools. Water molecules were removed (except the three water molecules HOH1034, HOH1066, HOH1183 present in the binding site) and H-atoms were added to the structure. Most likely positions of hydroxyl and thiol hydrogens, protonation states and tautomers of His residues, and Chi "flip" assignments for Asn, Gln and His residues were selected by the protein assignment script. Minimizations were performed until the average root mean square deviation of the non-hydrogen atoms reached 0.3 Å.

Preparation of compound libraries

The coordinates of nevirapine were obtained from the co-crystallized structure (1VRT and 3HVT). The other inhibitors for the target protein HIV-1 RT, p66 domain were built using the nevirapine as a template. The library of analogues was generated by modifying the respective functional groups (X, Y and R) in the scaffold structure with sterically and conformationally allowed substituents using the reagent database and the combinatorial design module (Schrödinger) (Table 1). Each structure was assigned an appropriate bond order using ligprep script shipped by Schrödinger. The inhibitors were converted to mae format (Maestro, Schrödinger Inc.) and optimized by means of the MMFF94 force field using default setting.

Table 1
Library of nevirapine analogues used in the work

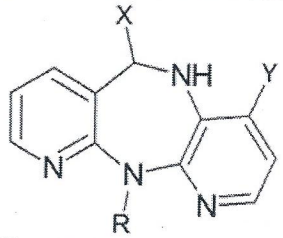

(Parental structure of Nevirapine)

Analogues	X	Y	R	Analogues	X	Y	R
S1(Original)	O	Cl	CYCLOPROPYL	S25	O	H	CYCLOPROPYL
S2	O	Cl	CYCLOPROPYL METHYL	S26	O	H	CYCLOPROPYL METHYL
S3	O	Cl	DIMETHYL ALLYL	S27	O	H	DIMETHYL ALLYL
S4	O	Cl	CH2-CO-CH3	S28	O	H	CH2-CO-CH3
S5	O	Cl	CH2-C(CH3)=CH2	S29	O	H	CH2-C(CH3)=CH2
S6	O	Cl	CH2C(CH=CH2)=CH2	S30	O	H	CH2C(CH=CH2)=CH2
S7	O	Cl	CH2COOCH3	S31	O	H	CH2COOCH3
S8	O	Cl	CH2CH2CH3	S32	O	H	CH2CH2CH3
S9	O	Cl	CH2CH2CH2CH3	S33	O	H	CH2CH2CH2CH3
S10	O	Cl	CH2CH2CH=CH2	S34	O	H	CH2CH2CH=CH2
S11	O	Cl	CH2CH=CHCH3	S35	O	H	CH2CH=CHCH3
S12	S	Cl	CH2C(CH3)=CHCH3	S36	O	H	CH2C(CH3)=CHCH3
S13	S	Cl	CYCLOPROPYL	S37	S	H	CYCLOPROPYL
S14	S	Cl	CYCLOPROPYL METHYL	S38	S	H	CYCLOPROPYL METHYL
S15	S	Cl	DIMETHYL ALLYL	S39	S	H	DIMETHYL ALLYL
S16	S	Cl	CH2-CO-CH3	S40	S	H	CH2-CO-CH3
S17	S	Cl	CH2-C(CH3)=CH2	S41	S	H	CH2-C(CH3)=CH2
S18	S	Cl	CH2C(CH=CH2)=CH2	S42	S	H	CH2C(CH=CH2)=CH2
S19	S	Cl	CH2COOCH3	S43	S	H	CH2COOCH3
S20	S	Cl	CH2CH2CH3	S44	S	H	CH2CH2CH3
S21	S	Cl	CH2CH2CH2CH3	S45	S	H	CH2CH2CH2CH3
S22	S	Cl	CH2CH2CH=CH2	S46	S	H	CH2CH2CH=CH2
S23	S	Cl	CH2CH=CHCH3	S47	S	H	CH2CH=CHCH3
S24	S	Cl	CH2C(CH3)=CHCH3	S48	S	H	CH2C(CH3)=CHCH3

Glide docking and scoring function

Glide calculations were performed with Impact version v18007 (Schrödinger, Inc.) [31–33]. It performs grid-based ligand docking with energetics and searches for favorable interactions between one or more typically small ligand molecules and a typically larger receptor molecule, usually a protein. Schrödinger recommends the performance of test calculations with different scaling factors for the receptor and ligand atom van der Waals radii, because steric repulsive interactions might otherwise be overemphasized, leading to rejection of overall correct binding modes of active compounds. After ensuring that protein and ligands are in correct form for docking, the receptor-grid files were generated using grid-receptor generation program. To soften the potential for nonpolar parts of the receptor, we scaled van der Waals radii of receptor atoms by 1.00 with partial atomic charge 0.25. A grid box of size $56 \times 56 \times 56$ points with coordinates $X = 3.4860$, $Y = -36.804$ and $Z = 22.3858$ was generated at the centroid of the active site and the size of ligands to be docked were selected from the workspace. The ligands were docked with the active site using the "xtra precision" Glide algorithm. Glide generates conformations internally and passes these through a series of filters. The first places the ligand center at

various grid positions of a 1 Å grid and rotates it around the three Euler angles. At this stage, crude score values and geometric filters weed out unlikely binding modes. The next filter stage involves a grid-based force field evaluation and refinement of docking solutions including torsional and rigid-body movements of the ligand. The OPLS-AA force field is used for this purpose. A small number of surviving docking solutions can then be subjected to a Monte Carlo procedure to minimize the energy score. The final energy evaluation is done with Glide score (*GScore*) and a single best pose is generated as the output for a particular ligand.

$$GScore = a * vdW + b * Coul + Lipo + Hbond + Metal + BuryP + RotB + Site$$

where *vdW* is van der Waals energy; *Coul*, Coulomb energy; *Lipo*, lipophilic contact term; *HBond*, hydrogen-bonding term; *Metal*, metal-binding term; *BuryP*, penalty for buried polar groups; *RotB*, penalty for freezing rotatable bonds; *Site*, polar interactions in the active site; and the coefficients of *vdW* and *Coul* are: $a = 0.065$, $b = 0.130$.

The choice of the best docked structure for each ligand was made using model energy score (*Emodel*) that combines Glide score, the nonbonded interaction energy and the excess internal energy of the generated ligand conformation. Glide computed the nonbonded interaction energy as a specially constructed Coulomb-van der Waals interaction-energy score (CvdW) that is formulated to avoid overlay rewarding charge-charge interactions at the expense of charge-dipole and dipole-dipole interactions. This score is intended to be more suitable for comparing the binding affinities of different ligands than is the 'raw' Coulomb-van der Waals interaction energy.

MM and binding free energies

For the calculation of free energy of binding (FEB) of the ligands with RT only the Glide-XP docking results was taken and only the best scoring pose for each ligand was taken into consideration. Bimolecular Association with Energetics (eMBrAcE) developed by Schrödinger was used for physics based rescoring procedure [27]. For each ligand, the protein-ligand complex ($E_{lig-prot}$), the free protein (E_{prot}), and the free ligand (E_{lig}) were all subjected to energy minimization in implicit solvent (generalized Born). eMBrAcE uses the OPLS-AA all-atom force field with the surface generalized Born implicit solvent model [34,35]. It uses traditional MM methods to calculate ligand-receptor interaction energies (G_{ele}, G_{vdW}, G_{solv}), with a Gaussian smooth dielectric constant function method [36] for electrostatic part of solvation energy and solvent-accessible surface for the nonpolar part of solvation energy. A conjugate gradient minimization protocol was used in all minimization. eMBrAcE minimization calculations were performed using energy difference mode, in which energy changes upon association are estimated, taking as input the complexes obtained after docking analysis (Glide outputs). The energy difference was calculated using the equation:

$$\Delta E = E_{complex} - E_{ligand} - E_{protein}$$

The full effects of relaxation and solvation are also included in this mode.

ADME screening

The QikProp program [37] was used to obtain the absorption, distribution, metabolism, and excretion (ADME) properties of the analogues. It predicts both physically significant descriptors and pharmaceutically relevant properties. All the analogues were neutralized before being used by Qikprop. The

Table 2
Information for RT crystal structures used in the study

PDB Code	Inhibitor	Resolution (Å)	*R*-value	No. of atoms
1VRT	Nevirapine	2.20	0.186	7953
3HVT	Nevirapine	2.90	0.266	7426

neutralizing step is essential, as in normal mode QikProp is unable to neutralize a structure and no properties will be generated. The program was processed in normal mode, predicting 44 properties for the 48 molecules which consisted of principal descriptors and the physiochemical properties with a detailed analysis of the predicted octanol/water partition coefficient (QPlogPo/w), predicted octanol/gas partition coefficient (QPlogPoct), predicted water/gas partition coefficient (QPlogPw), predicted polarizability in cubic angstroms (QPpolrz), % human oral absorption in intestine (QP%), predicted brain/blood partition coefficient (QPlogBB), predicted IC50 value for blockage of HERG K+ channels (log HERG), predicted skin permeability (QPlogKp), prediction of binding to human serum albumin (QPlogKhsa), predicted apparent Caco-2 cell permeability in nm/sec (QPPCaco) and predicted apparent MDCK cell permeability in nm/sec (QPPMDCK). Caco-2 cells are a model for the gut-blood barrier whereas MDCK cells are considered to be a good mimic for the blood-brain barrier. It also evaluates the acceptability of the analogues based on the Lipinski's rule of 5 (number of violations of Lipinski's rule of five) which is essential for rational drug design. Poor absorption or permeation are more likely when a ligand molecule violates Lipinski's rule of five i.e., has more than 5 hydrogen bond donors, the molecular weight is over 500, the log P is over 5 and the sum of N's and O's is over 10.

RESULTS AND DISCUSSION

Two PDB files (1VRT and 3HVT) of high resolution crystal structures of RT with nevirapine were used (Table 2) in the docking simulation. Visualization of the binding site of nevirapine revealed that the entrance to the active site varies in the two crystallographic structures. Two complexes of RT with co-crystallized nevirapine, PDB codes 1VRT and 3HVT were compared. When the nevirapine in these two complexes were superimposed, the root mean square deviation (RMSD) of the coordinates for the 187 atoms of residues, Leu100, Lys102, Lys103, Val179, Tyr188, Gly190, Phe227, Leu234 and His235, which form the binding site, is 1.5 Å, suggest that the active sites for these two complexes are not same.

Molecular docking of nevirapine and its analogues

The original crystal structures of 1VRT and 3HVT were used to validate the Glide-XP docking for the HIV-1 RT system. This was done by moving the inhibitor outside of active site entrance and then docking it back into the active site. The top 5 configurations after docking were taken into consideration to validate the result. The RMSD was calculated for each one in compare to the co-crystallized nevirapine. The RMSD value for 1VRT was found in between 0.55–2.2 Å while for 3HVT it was 0.43–1.01 Å (Table 3). This proved that the docked molecules were bound with similar orientation and conformation with the active site in RT.

To study the molecular basis of interaction and affinity of binding of the nevirapine and its analogues, all the ligands have been docked into the active site of RT. The docking result of these ligands was given in Table 4a and 4b. The ranking of ligands was done based on the Glide score. All the 48 ligands have accepted poses with both the receptors (1VRT and 3HVT). However, the energy difference among all the

Table 3
Docking result of five lowest configurations of nevirapine in reverse transcriptase (1VRT and 3HVT)

Configuration	Glide score	*Emodel* (kJ/mol)	ΔE^a	RMSD (Å)[b]
Docked in 1VRT				
1	−10.00	−286.5	0.0	0.55
2	−1.96	−281.3	−5.5	1.4
3	−1.83	−264.6	−16.7	1.4
4	−1.16	−249.5	−15.1	1.8
5	−0.09	−237.8	−11.7	2.2
Docked in 3HVT				
1	−12.74	−269.2	0.0	0.43
2	−12.68	−268.4	−0.8	0.54
3	−12.29	−267.1	−1.3	0.61
4	−11.73	−265.9	−1.2	0.90
5	−11.39	−255.8	−10.1	1.01

[a]$\Delta E = E_i - E_{lowest}$; [b]RMSD between docked and crystallographic nevirapine structures.

Table 4a
The docking results of nevirapine and its analogues in the original crystal structure of RT (1VRT) using Glide-XP

Rank	Ligand No.	Glide score	*Emodel* (kJ/mol)	Rank	Ligand No.	Glide score	*Emodel* (kJ/mol)
1	S48	−14.62	−252.05	25	S38	−12.41	−135.23
2	S17	−14.49	−207.25	26	S37	−12.46	−212.27
3	S42	−14.25	−186.73	27	S20	−12.25	−147.38
4	S47	−14.24	−210.18	28	S39	−12.19	−83.74
5	S24	−14.16	−201.39	29	S28	−12.17	−209.34
6	S41	−14.11	−257.07	30	S10	−12.13	−141.93
7	S43	−14.01	−301.87	31	S2	−11.99	−250.37
8	S13	−13.94	−244.93	32	S27	−11.25	−145.70
9	S16	−13.80	−246.18	33	S19	−11.17	−262.93
10	S21	−13.68	−231.11	34	S5	−10.96	−254.14
11	S45	−13.67	−238.65	35	S23	−10.95	−255.81
12	S22	−13.57	−243.25	36	S11	−10.43	−136.49
13	S18	−13.45	−146.12	37	S7	−10.19	−286.38
14	S44	−13.37	−218.55	38	S1(Nevirapine)	−10.00	−286.80
15	S36	−13.34	−208.08	39	S8	−9.90	−246.60
16	S14	−13.28	−237.81	40	S3	−9.82	−220.23
17	S40	−13.22	−216.04	41	S9	−9.64	−233.62
18	S46	−13.14	−149.05	42	S31	−8.87	−257.91
19	S12	−13.02	−162.87	43	S26	−8.85	−278.42
20	S4	−12.75	−129.79	44	S34	−8.70	−251.21
21	S15	−12.73	−32.24	45	S33	−8.68	−247.02
22	S35	−12.66	−109.69	46	S25	−8.52	−273.82
23	S29	−12.61	−239.48	47	S32	−8.52	−238.23
24	S6	−12.57	−143.61	48	S30	−6.33	−187.57

48 ligands is very small (+1.45 kJ/mol) in 3HVT compared to 1VRT (+3.54 kJ/mol). Minimum RMSD (0.89 Å) after superposition of docked nevirapine in 1VRT and 3HVT revealed that the binding mode of nevirapine in two RTs is considered to be essentially similar (Fig. 1a and 1b: Showing the docked nevirapine analogues in the active site of (a) reverse transcriptase 1 (1VRT) and (b) reverse transcriptase 1 (3HVT). Two stable hydrogen bonds (dotted green lines) formed between nevirapine and two water molecules in the binding site of RTs. By superposing the best binding conformation (with the lowest *Emodel* score of all the analogues; it is seen that these analogues bind in the same orientation and similar

Table 4b
The docking results of nevirapine and its analogues in the original crystal structure of RT (3HVT) using Glide-XP

Rank	Ligand No.	Glide score	*Emodel* (kJ/mol)	Rank	Ligand No.	Glide score	*Emodel* (kJ/mol)
1	S36	−15.26	−221.48	25	S45	−13.08	−140.68
2	S6	−14.64	−148.63	26	S46	−13.08	−175.85
3	S29	−14.22	−208.92	27	S40	−13.07	−218.13
4	S2	−13.94	−192.59	28	S39	−12.94	−133.14
5	S5	−13.92	−143.61	29	S7	−12.89	−271.30
6	S30	−13.88	−201.80	30	S47	−12.85	−130.21
7	S33	−13.77	−198.87	31	S32	−12.83	−162.87
8	S19	−13.54	−229.86	32	S22	−12.76	−170.40
9	S34	−13.52	−200.97	33	S1(Nevirapine)	−12.74	−269.21
10	S42	−13.50	−191.34	34	S41	−12.64	−169.57
11	S48	−13.49	−140.68	35	S21	−12.60	−154.49
12	S24	−13.48	−236.55	36	S4	−12.60	−184.22
13	S35	−13.43	−192.17	37	S43	−12.50	−198.04
14	S9	−13.43	−204.32	38	S31	−12.43	−246.60
15	S18	−13.41	−239.48	39	S8	−12.38	−195.10
16	S15	−13.31	−119.32	40	S14	−12.25	−40.61
17	S16	−13.29	−221.06	41	S20	−12.18	−123.09
18	S26	−13.28	−182.54	42	S11	−11.92	−188.82
19	S17	−13.24	−221.48	43	S44	−11.75	−133.56
20	S3	−13.22	−202.22	44	S37	−11.37	−126.02
21	S10	−13.17	−82.06	45	S23	−11.05	−147.79
22	S27	−13.14	−211.01	46	S38	−10.86	−65.73
23	S12	−13.12	−163.70	47	S13	−10.7	−93.78
24	S28	−13.08	−182.13	48	S25	−9.38	−171.66

position in terms of the common structure (triple-ring part) unlike that of nevirapine (Fig. 2a and 2b). As these molecules have the same backbone structure of the triple-ring, it is well possible that they bind in similar pattern in NNRTIs active site of RT in nature. All the 47 nevirapine analogues were found to be good binder with RT. The docking score (*GScore*) using Glide varies from −6.33 (analogue, S30) to a minimum of −14.62 (analogue, S48) in 1VRT and the score was −9.38 (analogue, S25) to −15.26 (analogue, S36) in 3HVT. Because the *GScore* for 3HVT is at the most negative range in compare to 1VRT, the binding site of 3HVT is the most accurate one for screening of most effective ligands. The co-crystallized nevirapine (S1) has docked score of −10.00 in 1VRT and −12.74 in 3HVT. Based on *GScore* it is revealed that the analogues of nevirapine prepared in this study could be the potential drugs for second generation drug development.

Calculated free energy of binding versus activity

For calculation of free energy of binding (FEB) and prediction of biological activity (pIC_{50}) only the docking simulation with 3HVT RT was taken into consideration. That was done because the RMSD value between the best five configurations of the nevirapine within the active site of 3HVT was much lower (1.01 Å) in comparison to 1VRT (2.2 Å) and revealed a better binding site. One docking structure with best poses (out of 5 poses with lowest Glide score) from each molecule docking result was used to calculate FEB using eMBrAcE (Schrödinger) and predicting IC_{50}. The interaction energy was calculated after a minimization was performed on a docked ligand in which atoms within 7.5 Å from the ligand were free to move (other atoms were fixed). The interaction energy includes an implicit solvation (H_2O) term. Van der Waals, solvation and electrostatic energy as well as solvent accessible surface area (SASA) were calculated for each minimized complex (Table 5). A similar scheme to linear response was used

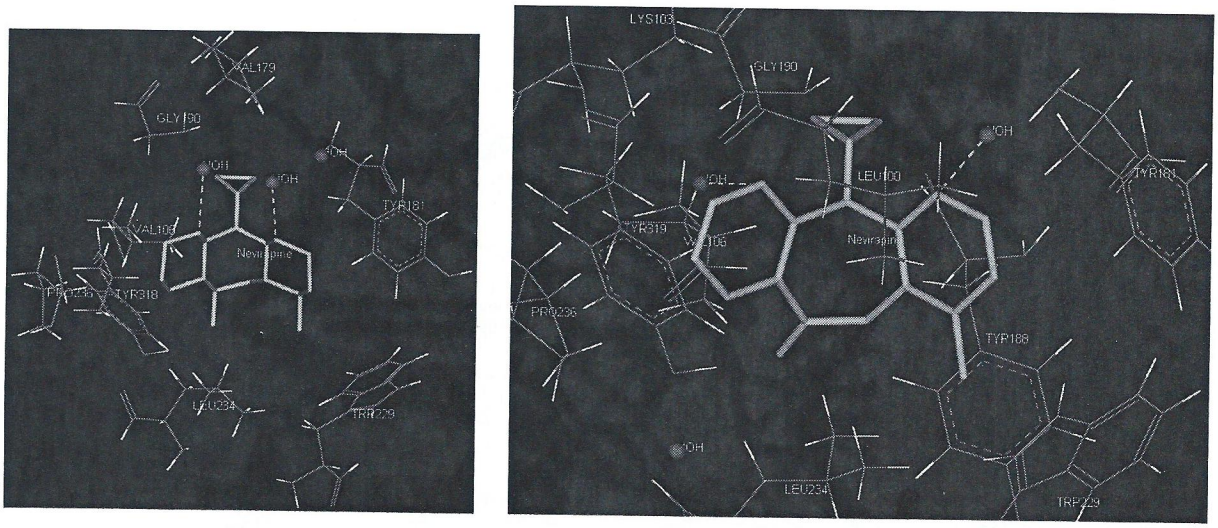

(a) (b)

Fig. 1. Showing the docked nevirapine analogues in the active site of (a) reverse transcriptase 1 (1VRT) and (b) reverse transcriptase 1 (3HVT). The green lines (dotted) demonstrate the hydrogen bonds formed between nevirapine and two water molecules within the binding site.

to develop a free energy of binding (FEB) relationship which in turn used to predict the activity (pIC_{50}) of nevirapine analogues. Theoretically, FEB can be partitioned into several components: van der Waals, electrostatic, solvation and entropy energy term. The entropy contribution is most difficult to calculate. However, several methods [38, 39] have been suggested to estimate the entropy contribution. For relatively rigid molecules, the entropy is relatively small and is normally ignored or cancelled in relative free energy calculation. Further, in the rational drug design, the calculation of relative FEB rather than absolute FEB is important. The plot of the FEB and log ($1/pIC_{50}$) reveals a significant relationship ($R^2 = 0.9948$) between these two parameters (Fig. 3). The linear trend in the plot indicated that the docking calculation produces reasonable binding modes. Based on correlation study, it is seen that electrostatic energy (G_{ele}) has most significant correlation to the activity (pIC_{50}) ($R^2 = 17\%$) followed by van der Waals energy ($R^2 = 12.5\%$), solvation energy ($R^2 = 7.9\%$) and SASA has list significant correlation ($R^2 = 0.1\%$) to the activity. It indicates that in the binding of nevirapine analogues, electrostatic energy estimated by GB/SA may be a major driving force to their binding and contribution to their activity. The calculated FEB among the ligands varies in between -20.70 to -38.42 kJ/mol and the overall difference is also very small (± 5.07 kJ/mol). It revealed that all these ligands bind in RT with high affinity and showed activity (pIC_{50}) in between 8.29 and 15.40. The co-crystallized ligand nevirapine having FEB -26.37 kJ/mol and pIC_{50} 10.57 proved to be less potent than that its analogues taken into consideration. The experimental IC_{50} value of nevirapine is 10.0 μM [40] which is very close to pIC_{50} and suggested that the calculated pIC_{50} based on FEB is robust and accurate.

ADME screening

We have analyzed 44 physically significant descriptors and pharmaceutically relevant properties of nevirapine and its analogues, among which were molecular weight, polarizability (Å), log P (octanol/gas), log P (water/gas), log P (octanol/water), log BB (brain/blood), log P MDCK, log Kp (skin permeability),

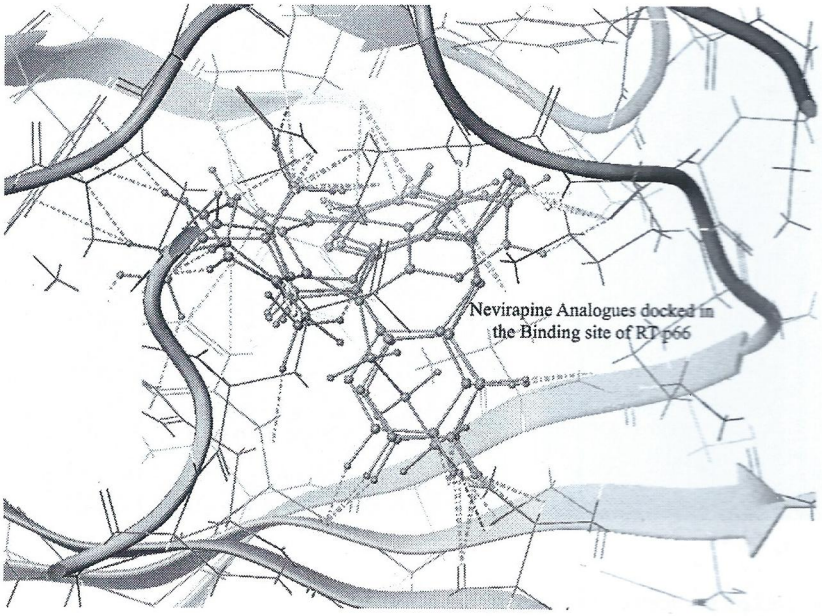

(a)

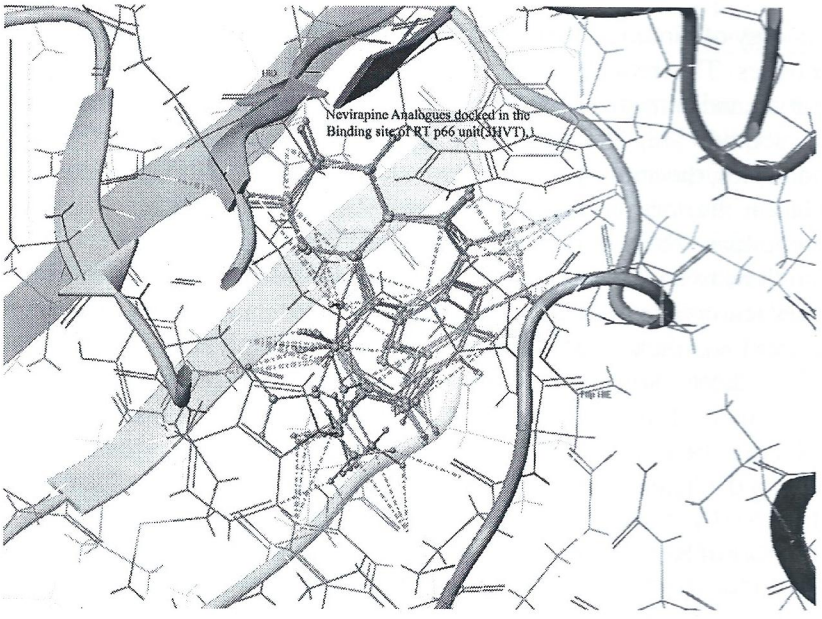

(b)

Fig. 2. Showing the superposition of six lowest energy configurations of nevirapine analogues docked in (a) reverse transcriptase 1 (1VRT) and (b) reverse transcriptase 1 (3HVT).

log Khsa (serum protein binding) etc. and their screening in accordance to Lipinski's rule of 5. For the log P (octanol/water), QP%, and log HERG, if the value for a utilized descriptor exceeded the range for the experimental training set, it was flagged. In this study out of 48 ligands, all the structures showed

Table 5
Calculated energies and estimated free energy of binding (FEB) of nevirapine and its analogues (kJ/mol) in RT (3HVT)

Analogues	G_{vdw}	G_{ele}	G_{solv}	SASA	FEB1	pIC_{50}^2	Analogues	G_{vdw}	G_{ele}	G_{solv}	SASA	FEB[1]	pIC_{50}^2
S1	−58.55	18.24	13.94	503.05	−26.37	10.57	S25	−66.52	31.05	−9.85	473.87	−32.32	12.95
S2	−49.77	−0.70	29.29	528.71	−21.18	8.49	S26	−51.55	−28.22	43.29	499.61	−36.48	14.62
S3	−61.85	18.74	13.59	551.51	−29.52	11.83	S27	−56.35	−28.32	43.14	520.92	−32.53	13.04
S4	−74.38	18.78	9.79	502.38	−25.81	10.34	S28	−75.75	18.63	5.10	475.67	−32.02	12.83
S5	−52.80	−5.56	24.73	521.84	−33.63	13.48	S29	−61.32	33.82	−9.13	494.42	−36.63	14.68
S6	−59.39	17.12	12.97	536.93	−29.30	11.74	S30	−49.66	8.82	5.84	508.01	−35.00	14.03
S7	−72.86	−21.73	32.28	540.62	−33.31	13.35	S31	−71.97	−46.92	57.41	498.20	−35.48	14.22
S8	−71.29	−2.63	38.42	516.36	−35.50	14.23	S32	−65.52	27.45	−11.85	488.83	−33.74	13.52
S9	−78.29	−7.69	42.02	548.39	−33.96	13.61	S33	−71.01	−5.47	26.90	521.50	−29.58	11.85
S10	−73.40	6.36	20.97	536.48	−33.07	13.25	S34	−51.27	−21.33	48.56	508.01	−24.04	9.63
S11	−67.42	−29.65	49.10	536.76	−31.97	12.81	S35	−56.67	2.26	27.30	510.83	−27.11	10.86
S12	−75.46	−22.61	45.12	548.71	−35.10	14.07	S36	−55.29	−27.48	11.56	520.30	−33.21	13.31
S13	−63.99	2.49	27.00	517.59	−34.50	13.83	S37	−65.98	−17.32	34.01	491.48	−29.29	11.74
S14	−74.86	−21.63	29.28	542.49	−35.21	14.11	S38	−50.23	−9.23	21.54	516.37	−23.92	9.59
S15	−79.73	9.98	13.16	569.64	−26.59	10.66	S39	−76.13	−0.05	29.32	545.28	−26.86	10.76
S16	−54.85	−28.50	46.04	520.22	−37.31	14.95	S40	−40.65	−12.52	32.47	495.95	−20.70	8.29
S17	−73.88	−20.73	32.22	543.14	−33.39	13.38	S41	−58.76	15.66	20.17	512.10	−22.93	9.19
S18	−57.02	7.87	6.42	558.40	−22.73	9.11	S42	−71.63	−13.52	31.87	532.87	−33.28	13.34
S19	−69.86	−20.43	30.28	540.01	−34.01	13.63	S43	−62.55	4.69	21.65	516.50	−36.21	14.51
S20	−64.68	35.65	3.51	531.32	−25.52	10.23	S44	−61.96	21.72	17.29	505.56	−22.95	9.20
S21	−61.83	36.35	0.99	564.04	−24.49	9.81	S45	−76.32	−16.85	43.29	537.81	−34.88	13.98
S22	−53.27	−3.43	21.08	553.82	−35.62	14.28	S46	−36.06	5.06	3.18	525.14	−27.82	11.15
S23	−61.13	14.82	2.77	554.46	−23.54	9.43	S47	−56.35	20.38	7.40	530.21	−28.57	11.45
S24	−70.04	−31.25	47.87	562.18	−38.42	15.40	S48	−55.09	11.24	22.28	534.23	−21.57	8.64

1. Calculated free energy of binding, ΔG_{cald} is calculated from optimized linear combination of ΔG_{ele}, ΔG_{vdW}, ΔG_{solv}, and SASA from regression.
2. Predicted pIC_{50} is estimated from ΔG_{cald} using the following relationship: $\Delta G_{binding} = RT\ln K_{dissociated} \approx RT\ln IC_{50} = -RTpIC_{50}$, where temperature ($T$) = 300 Kelvin.

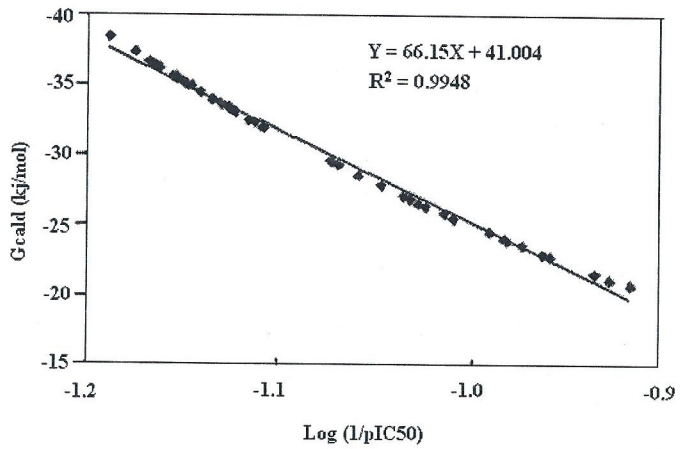

Fig. 3. Linear regression plot between FEB and log ($1/pIC_{50}$) of 48 nevirapine analogues used in the study.

Table 6
Screening of ADME properties for nevirapine and its analogues using Qikprop simulation

Ligand No.	QP logPo/w	QP %	Log HERG	QPP Caco	QPP MDCK	Rule of 5	Ligand No.	QP logPo/w	QP %	Log HERG	QPP Caco	QPP MDCK	Rule of 5
S1	2.41	96.45	−4.70	2394.58	1271.31	0	S25	2.04	96.16	−4.70	1807.54	938.06	0
S2	2.77	100	−4.81	2571.59	1373.19	0	S26	2.39	96.91	−4.82	1949.94	1018.19	0
S3	3.14	100	−4.93	2799.13	1504.97	0	S27	2.77	100	−4.90	2198.28	1159.05	0
S4	2.55	100	−4.85	2784.29	1496.35	0	S28	2.17	100	−4.92	2118.26	1113.51	0
S5	2.78	100	−4.77	2504.50	1334.50	0	S29	2.40	100	−4.82	1873.94	975.36	0
S6	3.08	100	−4.91	2597.04	1387.88	0	S30	2.70	100	−4.94	2067.76	1084.84	0
S7	1.72	86.78	−5.04	973.11	480.34	0	S31	1.30	86.07	−4.78	716.24	344.89	0
S8	2.64	100	−4.85	2851.69	1535.54	0	S32	2.25	100	−4.90	2156.90	1135.48	0
S9	3.00	100	−5.08	2849.09	1534.03	0	S33	2.61	100	−5.15	2150.99	1132.12	0
S10	2.95	100	−5.14	2845.18	1531.75	0	S34	2.56	100	−5.17	2159.78	1137.12	0
S11	2.89	100	−5.02	2791.90	1500.77	0	S35	2.51	100	−5.12	2107.86	1107.60	0
S12	3.11	96.90	−4.80	2478.48	1319.52	0	S36	2.70	96.66	−4.86	1892.64	985.89	0
S13	3.84	100	−4.71	6587.48	9162.24	0	S37	3.46	100	−4.80	5166.99	7132.53	0
S14	4.20	100	−4.81	7106.21	9946.96	0	S38	3.82	100	−4.90	5597.36	7777.39	0
S15	4.57	100	−4.99	7349.06	10000	0	S39	4.21	100	−5.13	5908.02	8126.54	0
S16	3.96	100	−4.91	7266.95	9958.89	0	S40	3.60	100	−5.06	5871.30	8071.45	0
S17	4.21	100	−4.91	6116.45	8345.31	0	S41	3.85	100	−4.91	5484.99	7557.75	0
S18	4.46	100	−5.11	6081.60	7942.00	0	S42	4.10	100	−5.21	4890.80	6434.53	0
S19	3.04	96.366	−4.74	2450.63	3081.45	0	S43	2.70	96.97	−4.89	1984.80	2517.40	0
S20	4.03	100	−4.86	7353.41	10000	0	S44	3.68	100	−4.98	6222.04	8582.52	0
S21	4.41	100	−5.10	7354.26	10000	0	S45	4.05	100	−5.22	6233.76	8593.73	0
S22	4.35	100	−5.20	7260.14	9909.77	0	S46	4.00	100	−5.26	6278.26	8663.16	0
S23	4.32	100	−5.07	7269.83	9968.77	0	S47	3.95	100	−5.22	5871.27	8072.30	0
S24	4.49	100	−4.80	6118.09	7923.95	0	S48	4.14	100	−4.87	5460.32	7193.08	0

QP logPo/w – QP log P for octanol/water. QP % – % Human oral absorption in GI (+−20%) (<25% is poor). log HERG – HERG K+ channel blockage (concern below −5). QPP Caco – Apparent Caco-2 permeability (nm/sec) (<25 poor, >500 great). Qpp MDCk – Apparent MDCK permeability (nm/sec) (<25 poor, >500 great). Rule of 5 – Lipinski Rule of 5 violations.

significant values for the properties analyzed and showed drug like characteristic's based on Lipinski's rule of 5 (Table 6).

Biological indications of docking structure and ADME screening

The naturally occurring and the synthetic compounds (Table 1) were evaluated using docking-MM-GB/SA approach. The docking results showed that the structurally homologous inhibitors bind in a very similar position and orientation to RT, which suggests that the homologous inhibitors have similar binding patterns and interaction modes in RT, and further have similar inhibitory mechanism. Furthermore, the most potent inhibitor should have the interaction with the highest affinity with RT.

The docking structures of all compounds showed that they bind in very similar pattern in RT unlike that of nevirapine. To illustrate the binding structures of compounds of different activity, we superpose six higher activity ligands (S36,S6,S29,S2) and two lower activity ligands (S12,S28) docked into the active site of 3HVT (Fig. 4). For sake of clarity we did not put all ligands on the figure. The calculated FEB of the 47 nevirapine analogues demonstrates a linear correlation ($R^2 = 0.9944$) with their log ($1/\text{pIC}_{50}$) value. This concludes that the structural modification implemented in this study is significantly related to their activity. Also this proved the reasonability and reliability of the docking results. It can be seen that substitution of functional groups at position X, Y and R leads to increase in binding affinity of modified analogues even more intense than that of co-crystallized ligand. For example substitution of O, H and $CH_2C(CH_3) = CHCH_3$ at X, Y and R position in the scaffold structure of nevirapine obtained

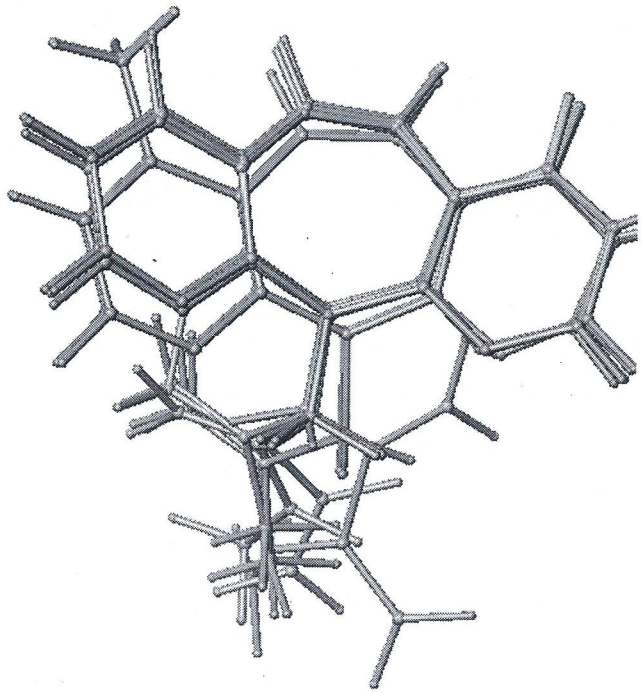

Fig. 4. Showing the superposition of six higher activity ligands (S36, S6, S29, S2) and two lower activity ligands (S12, S28) docked into the active site of 3HVT.

the best result with docking score $= -15.26$, FEB $= -33.21$ kJ/mol and $pIC_{50} = 13.21$. Further ADME screening provided a peered analysis for the final selection of the potential candidates from the compound library generated. Based on the overall analysis we can conclude that the analogues S36 and S29 are the most potent analogues which could be used for second generation of drug development. Both have exhibited effective binding in the active site of RT, showed an optimal predicted IC_{50} values and even qualify the Lipinski's rule of five.

The combined approach of docking-MM-GB/SA and the final screening based on ADME properties used in this work has the potential to predict the binding affinity of a large set of ligands to a receptor as well as their validation as potential drug candidates for second generation drug discovery.

REFERENCES

[1] Arnold, E. and Jacobo-Molina, A. (1991). HIV reverse transcriptase structure-function relationships. Biochemistry **30**, 6351-6361.

[2] Le Grice, S. F. J. (1993). Human immunodeficiency virus reverse transcriptase. *In:* Reverse transcriptase, Skalka, A. M. and Goff, S. P. (eds.), Cold Spring Harbor Laboratory Press, Cold Spring Harbor, NY, pp. 163-191.

[3] Goff, P. (1990). Retroviral reverse transcriptase: Synthesis, structure and function. J. Acquir. Immune Defic. Syndr. **3**, 817-831.

[4] Whitcomb, J. M. and Hughes, S. H. (1992). Retroviral reverse transcription and integration: Progress and problems. Annu. Rev. Cell Biol. **8**, 275-306.

[5] Huang, H., Chopra, R., Verdine, G. L. and Harrison, S. C. (1998). Structure of a covalently trapped catalytic complex of HIV-1 reverse transcriptase: implications for drug resistance. Science **282**, 1669-1675.

[6] Tantillo, C., Ding, J., Jacobo-Molina, A., Nanni, R. G., Boyer, P. L., Hughes, S. H., Pauwels, R., Andries, K., Janssen, P. A. J. and Arnold, E. (1994). Locations of anti-AIDS drug binding sites and resistance mutations in the three-dimensional

structure of HIV-1 reverse transcriptase. Implications for mechanisms of drug inhibition and resistance. J. Mol. Biol. **243**, 369-387.

[7] Kohlstaedt, L. A., Wang, J., Friedman, J. M., Rice, P. A. and Steitz, T. A. (1992). Crystal structure at 3.5 Å resolution of HIV-1 reverse transcriptase complexed with an inhibitor. Science **256**, 1783-1790.

[8] Smerdon, S. J., Jäger, J., Wang, J., Kohlstaedt, L. A., Chirino, A. J., Friedman, J. M., Rice, P. A. and Steitz, T. A. (1994). Structure of the binding site for nonnucleoside inhibitors of the reverse transcriptase of human immunodeficiency virus type 1. Proc. Natl. Acad. Sci. USA **91**, 3911-3915.

[9] Ding, J., Das, K., Moereels, H., Koymans, L., Andries, K., Janssen, P. A., Hughes, S. H. and Arnold, E. (1995). Structure of HIV-1 RT/TIBO R 86183 complex reveals similarity in the binding of diverse nonnucleoside inhibitors. Nat. Struct. Biol. **2**, 407-415.

[10] Jacobo-Molina, A., Ding, J., Nanni, R. G., Clark, A. D. Jr., Lu, X., Tantillo, C., Williams, R. L., Kamer, G., Ferris, A. L., Clark, P., Hizi, A., Hughes, S. H. and Arnold, E. (1993). Crystal structure of human immunodeficiency virus type 1 reverse transcriptase complexed with double-stranded DNA at 3.0 Å resolution shows bent DNA. Proc. Natl. Acad. Sci. USA **90**, 6320-6324.

[11] Garg, R., Gupta, S. P., Gao, H., Babu, M. S., Debnath, A. K. and Hansch, C. (1999). Comparative quantitative structure-activity relationship studies on anti HIV drugs. Chem. Rev. **99**, 3525-3602.

[12] Arnold, E., Das, K., Ding, J., Yadav, P. N., Hsiou, Y., Boyer, P. L. and Hughes, S. H. (1996). Targeting HIV reverse transcriptase for anti-AIDS drug design: structural and biological considerations for chemotherapeutic strategies. Drug Des. Discov. **13**, 29-47.

[13] Larder, B. A. (1993). Inhibitors of HIV reverse transcriptase as antiviral agents and drug resistance. *In:* Reverse transcriptase, Skalka, A. M. and Goff, S. P. (eds.), Cold Spring Harbor Laboratory Press, Cold Spring Harbor, NY, pp. 205-222.

[14] De Clercq, E. (1995). Antiviral therapy for human immunodeficiency virus infections. Clin. Microbiol. Rev. **8**, 200-239.

[15] Ding, J., Das, K., Ydev, P. N. S., Hsiou, Y., Zhang, W., Hughes, S. H. and Arnold, E. (1997). Structural studies of HIV-1 reverse transcriptase and implications for drug design. *In:* Structure based drug design, Veerapandian, P. (ed.), Marcel Dekker, New York, pp. 41-82.

[16] Pedersen, O. S. and Pedersen, E. B. (1999). Non-nucleoside reverse transcriptase inhibitors: the NNRTI boom. Antivir. Chem. Chemother. **10**, 285-314.

[17] Ding, J., Hughes, S. H. and Arnold, E. (1997). Protein-nucleic acid interactions and DNA conformation in a complex of human immunodeficiency virus type 1 reverse transcriptase with a double-stranded DNA template-primer. Biopolymers **44**, 125-138.

[18] Hsiou, Y., Ding, J., Das, K., Clark, A. D. Jr., Hughes, S. H. and Arnold, E. (1996). Structure of unliganded HIV-1 reverse transcriptase at 2.7 Å resolution: implications of conformational changes for polymerization and inhibition mechanisms. Structure **4**, 853-860.

[19] Jäger, J., Smerdon, S. J., Wang, J., Boisvert, D. C. and Steitz, T. A. (1994). Comparison of three different crystal forms shows HIV-1 reverse transcriptase displays an internal swivel motion. Structure **2**, 869-876.

[20] Ren, J., *et al.* (1995). High resolution structures of HIV-1 RT from four RT-inhibitor complexes. Nat. Struct. Biol. **2**, 293-302.

[21] Wang, J., Smerdon, S. J., Jäger, J., Kohlstaedt, L. A., Rice, P. A., Friedman, J. M. and Steitz, T. A. (1994). Structural basis of asymmetry in the human immunodeficiency virus type 1 reverse transcriptase heterodimer. Proc. Natl. Acad. Sci. USA **91**, 7242-7246.

[22] Koup, R. A., Merluzzi, V. J., Hargrave, K. D., Adams, J., Grozinger, K., Eckner, R. J. and Sullivan, J. L. (1991). Inhibition of human immunodeficiency virus type1 replication by the dipyridocliazepinone BI-RG-587. J. Infect. Dis. **163**, 966-970.

[23] Richman, D., Rosenthal, A. S., Skoog, M., Eckner, R. J., Chou, T. C., Sabo, J. P. and Merluzzi, V. J. (1991). BI-RG-587 in active against zidovudine-resisant human immunodedeficiency virus type 1 and synergistic with zidovudine. Antimicrob. Agents Chemother. **35**, 305-308.

[24] Kroeger Smith, M. B., Lamb, M. L., Tirado-Rives, J., Jorgensen, W. L., Michejda, C. J., Ruby, S. K. and Smith, R. H. Jr. (2000). Monte Carlo calculations on HIV-1 reverse transcriptase complexed with the non-nucleoside inhibitor 8-Cl TIBO: contribution of the L100I and Y181C variants to protein stability and biological activity. Protein Eng. **13**, 413-421.

[25] Wang, J., Morin, P., Wang, W. and Kollman, P. A. (2001). Use of MM-PBSA in reproducing the binding free energies to HIV-1 RT of TIBO derivatives and predicting the binding mode to HIV-1 RT of efavirenz by docking and MM-PBSA. J. Am. Chem. Soc. **123**, 5221-5230.

[26] Smith, P. A., Sorich, M. J., Low, L. S. C., McKinnon, R. A. and Miners, J. O. (2004). Towards integrated ADME prediction: past, present and future directions for modelling metabolism by UDP-glucuronosyltransferases. J. Mol. Graph. Model. **22**, 507-517.

[27] Guvench, O., Weiser, J., Shenkin, P. S., Kolossváry, I. and Still, W. C. (2002). Application of the frozen atom approximation to the GB/SA continuum model for solvation free energy. J. Comput. Chem. **23**, 214-221.

[28] Still, W. C., Tempczyk, A., Hawley, R. C. and Hendrickson, T. (1990). Semianalytical treatment of solvation for molecular mechanics and dynamics. J. Am. Chem. Soc. **112**, 6127-6129.

[29] Qiu, D., Shenkin, P. S., Hollinger, F. P. and Still, W. C. (1997). The GB/SA continuum model for solvation. A fast analytical method for the calculation of approximate Born radii. J. Phys. Chem. **101**, 3005-3014.

[30] Hasel, W., Hendrickson, T. F. and Still, W. C. (1988). A rapid approximation to the solvent accessible surface areas of atoms. Tetrahedron Comput. Method. **1**, 103-116.

[31] Halgren, T. A., Murphy, R. B., Friesner, R. A., Beard, H. S., Frye, L. L., Pollard, W. T. and Banks, J. L. (2004). Glide: A new approach for rapid, accurate docking and scoring. 2. Enrichment factors in database screening. J. Med. Chem. **47**, 1750-1759.

[32] Krovat, E. M., Steindl, T. and Langer, T. (2005). Recent advances in docking and scoring. Current Computer-Aided Drug Design **1**, 93-102.

[33] Friesner, R. A., Banks, J. L., Murphy, R. B., Halgren, T. A., Klicic, J. J., Mainz, D. T., Repasky, M. P., Knoll, E. H., Shelley, M., Perry, J. K., Shaw, D. E., Francis, P. and Shenkin, P. S. (2004). Glide: A new approach for rapid, accurate docking and scoring. 1. Method and assessment of docking accuracy. J. Med. Chem. **47**, 1739-1749.

[34] Wu, X., Milne, J. L. S., Borgnia, M. J., Rostapshov, A. V., Subramaniam, S. and Brooks, B. R. (2003). A core-weighted fitting method for docking atomic structures into low-resolution maps: application to cryo-electron microscopy. J. Struct. Bio. **141**, 63-76.

[35] Todorov, N. P., Mancera, R. L. and Monthoux, P. H. (2003). A new quantum stochastic tunnelling optimisation method for protein-ligand docking. Chemical Physics Letters **369**, 257-263.

[36] Reynolds, C. H. (1995). Estimating liphophilicity using GB/SA continuum solvation Model: a direct method for computing partition coefficients. J. Chem. Inf. Comput. Sci. **35**, 738-742.

[37] Duffy, E. M. and Jorgensen, W. L. (2000). Prediction of Properties from Simulations: Free Energies of Solvation in Hexadecane, Octanol, and Water. J. Am. Chem. Soc. **122**, 2878-2888.

[38] Wang, W., Lim, W. A., Jakalian, A., Wang, J., Luo, R., Bayly, C. L. and Kollman, P. A. (2001). An analysis of the interactions between the Sem-5 SH3 domain and its ligands using molecular dynamics, free energy calculation and sequence analysis. J. Am. Chem. Soc. **123**, 3986-3994.

[39] Zhou, Z., Fisher, D., Spidel, J., Greenfield, J., Patson, B., Fazal, A., Wigal, C., Moe, O. A. and Madura, J. D. (2003). Kinetic and docking studies of the interaction of quinones with the quinone reductase active site. Biochemistry **42**, 1985-1994.

[40] Iglesias-Ussel, M. D., Casado, C., Yuste, E., Olivares, I. and López-Galíndez, C. (2002). *In vitro* analysis of human immunodeficiency virus type 1 resistance to nevirapine and fitness determination of resistant variants. J. Gen. Virol. **83**, 93-101.